Enhanced charge photogeneration promoted by crystallinity in small-molecule donor-acceptor bulk heterojunctions

Keshab Paudel, Brian Johnson, Mattson Thieme, Michael M. Haley, Marcia M. Payne, John E. Anthony, and Oksana Ostroverkhova

Articles you may be interested in

Enhanced charge collection in confined bulk heterojunction organic solar cells
Appl. Phys. Lett. **99**, 163301 (2011); 10.1063/1.3651509

Energy level alignments and photocurrents in crystalline Si/organic semiconductor heterojunction diodes
J. Appl. Phys. **106**, 113704 (2009); 10.1063/1.3264945

Dramatic enhancement of photo-oxidation stability of a conjugated polymer in blends with organic acceptor
Appl. Phys. Lett. **92**, 243311 (2008); 10.1063/1.2945801

Charge carrier generation and electron blocking at interlayers in polymer solar cells
Appl. Phys. Lett. **90**, 133502 (2007); 10.1063/1.2715029

Hole injection barriers at polymer anode/small molecule interfaces
Appl. Phys. Lett. **79**, 557 (2001); 10.1063/1.1386400

Enhanced charge photogeneration promoted by crystallinity in small-molecule donor-acceptor bulk heterojunctions

Keshab Paudel,[1] Brian Johnson,[1] Mattson Thieme,[1] Michael M. Haley,[2] Marcia M. Payne,[3] John E. Anthony,[3] and Oksana Ostroverkhova[1,a)]

[1]Department of Physics, Oregon State University, Corvallis, Oregon 97331, USA
[2]Department of Chemistry and Biochemistry, University of Oregon, Eugene, Oregon 97403, USA
[3]Department of Chemistry, University of Kentucky, Lexington, Kentucky 40506, USA

We examined sub-nanosecond time-scale charge carrier dynamics in crystalline films of a functionalized anthradithiophene (ADT) donor (D) with three different acceptor (A) molecules. A four-fold enhancement in ultrafast charge carrier separation efficiency was observed in D/A blends with a fullerene acceptor added at 7–10 wt. % concentrations, whereas a gradual decrease in peak photocurrent amplitude with acceptor concentration was observed with functionalized pentacene and indenofluorene acceptors. The results were directly correlated with the ADT-tri(ethylsilyl)ethynyl-F donor crystallinity. In the best-performing blends, the presence of crystalline acceptor domains was also established. © 2014 AIP Publishing LLC. [http://dx.doi.org/10.1063/1.4891758]

Organic semiconductors are of interest due to their potential applications in low-cost, solution-processable, and light-weight (opto)electronic devices.[1] An important subset of these applications, e.g., solar cells, photodetectors, and photorefractive devices, relies on efficient photoinduced charge carrier generation. A common way of improving charge photogeneration efficiency in organic materials involves creating donor-acceptor (D/A) bulk heterojunctions (BHJs), in which charge separation occurs via electron (hole) transfer from the photo-excited donor (acceptor) to acceptor (donor).[2] Considerable research efforts have been devoted to understanding charge generation in polymer/fullerene BHJs[2] and, more recently, in small-molecule BHJs.[3–10] Currently, the best-performing BHJs involve fullerene acceptors, which have significant drawbacks, and the quest for high-performance non-fullerene acceptors remains open.[11–14] Given that fullerenes exhibit a range of properties that could be favorable for charge carrier photogeneration (including high electron affinity, good electron transport properties, structure and morphology enabling 3D transport, and availability of several closely spaced excited states that can accept electrons),[4,13] it is important to establish the most critical properties driving charge photogeneration processes in particular D/A systems. In this Letter, we quantify charge photogeneration processes in organic small-molecule D/A BHJs with a functionalized anthradithiophene (ADT) derivative as the donor and three different types of acceptors. We combine measurements of transient photocurrent (TPC), photoluminescence (PL), and x-ray diffraction (XRD) with numerical modeling to establish the dominant factor in fast charge carrier photogeneration.

For our study, we chose a fluorinated ADT derivative functionalized with tri(ethylsilyl)ethynyl (TES) side groups, ADT-TES-F (Fig. 1(a)), as the donor. ADT-TES-F exhibits 2D "brick-work" π-stacking and forms crystalline films characterized by hole mobilities reaching 1.5 cm²/(Vs) in spin-cast thin-film transistors,[15,16] fast charge carrier photogeneration, and

high photoconductive gains.[8,17] A fluorinated pentacene (Pn) derivative functionalized with tri(isopropylsilyl)ethynyl (TIPS) side groups, Pn-TIPS-F8 (Fig. 1(b)), an indeno[2,1-c]fluorene derivative, indenofluorene (IF)-Mes (Fig. 1(c)),[18] or [6,6]-Phenyl C_{61} butyric acid methyl ester, PCBM (Fig. 1(d)), were used as acceptors. The choice of the acceptor molecules was guided by the following considerations. Pn-TIPS-F8 and IF-Mes molecules have similar LUMO energy levels (Fig. 1(e)), which yield D/A LUMO energy offsets of ∼0.55 eV. (Such offsets should favor high power conversion efficiencies,[19,20] although the validity of quantitative assessments of the photo-induced charge transfer (CT) efficiency based on this characteristic has been debated in the literature.[21]) However, these two molecules exhibit considerably different solid-state packing motifs and excited state dynamics, properties known to affect CT and charge generation, thus creating different scenarios for photoexcitation relaxation pathways in D/A blends with these acceptors.[22] In particular, the Pn-TIPS-F8 exhibits 2D "brick-work" π-stacking (similar to ADT-TES-F) in the solid state, it is fluorescent and, when blended with the ADT-TES-F donor, an emissive CT state (exciplex) with a lifetime of ∼4 ns forms.[6,7] In contrast, IF-Mes does not yield π-stacked structures,[18] and it is non-fluorescent due to fast non-radiative
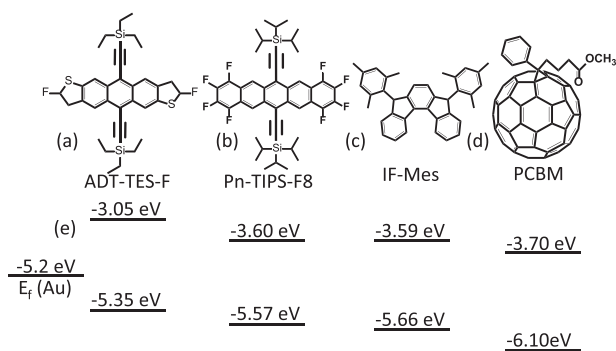

FIG. 1. (a)–(d) Molecular structures and (e) HOMO and LUMO energies of molecules used in this study. The work function of gold is included for reference.

a)Electronic mail: ostroveo@science.oregonstate.edu

relaxation. For comparison, D/A blends with the fullerene acceptor PCBM commonly utilized in organic BHJs were also studied.

In order to prepare samples, 30 mM toluene solutions of donor and acceptor molecules were mixed in appropriate proportions to achieve acceptor concentrations in the D/A films ranging between 0 and 20–40 wt. %, depending on the acceptor. Films were then spin-cast out of these solutions at 3000 rpm, at room temperature, onto glass substrates pre-patterned with Cr/Au (5 nm/50 nm thick) interdigitated electrodes with a finger length and width of 1 mm and 25 μm, respectively, and a 25 μm gap between adjacent fingers.[7] Each substrate was also pre-treated with a pentafluorobenzenethiol (PFBT) solution, to facilitate crystallization.[16] Optical absorption and PL properties of the films can be found in the supplementary material (Figs. S1–S3).[23]

In order to establish the effect of acceptor addition on fast charge carrier photogeneration, we measured time-resolved TPC under a pulsed 532 nm excitation (470 ps, 55 kHz, Q-switched frequency doubled Nd:YAG laser, Altechna STA-01-SH-4-MOPA) at a fluence of ∼2.0 μJ/cm^2. Voltage was applied to the samples using a Keithley 237 source-measure unit, and transient photocurrents were measured using a 50 GHz digital sampling oscilloscope (Tektronix CSA8000) with a time resolution of ∼0.6 ns limited by the laser pulse width and jitter.[6–9,17]

TPCs obtained in a pristine ADT-TES-F film and several D/A blends are shown in Figs. 2(a), S4, and S5. Fast photocurrent rise was observed in all samples, regardless of the type of acceptor or its concentration. As shown in Fig. 2(b), D/A films with Pn-TIPS-F8 and IF-Mes acceptors exhibited peak photocurrent amplitudes (I_{pk}) gradually decreasing as acceptor concentration increased.[7] In contrast, in ADT-TES-F/PCBM films, I_{pk} increased with PCBM concentration up to ∼7–10 wt. %, reaching values a factor of ∼4 higher than those in pristine ADT-TES-F films, and then decreased at higher concentrations (Fig. 2(b)). Additionally, the initial decay of

the photocurrent in ADT-TES-F/PCBM blends was considerably faster than that in pristine donor films and in D/A films with Pn-TIPS-F8 or IF-Mes acceptors (Fig. 2(a)), due to bimolecular recombination (Fig. S6). Similar trends in both the photocurrent amplitude and decay dynamics were previously observed in ADT-TES-F/C_{60} films.[8,9]

In order to gain physical insight into charge carrier dynamics in our D/A blends, we performed numerical simulations of the TPC following a previously reported approach,[10] which has been modified to incorporate a correction[24] to the Onsager-Braun model.[25] This enabled us to quantify the distribution of photoexcitation among several relaxation pathways, depending on the acceptor. In our model, charge photogeneration may proceed via (i) ultrafast creation of spatially separated charge carriers (SSCs) (via, for example, band-to-band transitions, hot exciton dissociation, and/or any other process occurring on sub-ps time scales), (ii) Frenkel exciton (FE) dissociation, and (iii) CT exciton dissociation. The presence of CT excitons was directly confirmed in ADT-TES-F/Pn-TIPS-F8 D/A blends via PL emission from the ADT-TES-F/Pn-TIPS-F8 exciplex centered at ∼715 nm (Fig. S2(a)), as detailed in previous studies.[6,7] PL emission in ADT-TES-F/IF-Mes and ADT-TES-F/PCBM films was solely due to residual emission from the ADT-TES-F donor (Figs. S2(b) and S2(c)). However, this does not necessarily indicate the absence of CT state formation in these D/A films; for example, dark CT state formation between ADT-TES-F and PCBM has been previously inferred from TPC.[6,10] Thus, the possibility of CT excitons contributing to charge photogeneration was included in our simulations for all D/A blends. The efficiency of the ultrafast channel is characterized by a parameter ξ_{SSC} (which represents the fraction of absorbed photon density that results in SSCs on ultrafast time scales). The parameters of interest for the other two charge photogeneration channels are $\xi_{FE}\eta_{FE}$ and $\xi_{CT}\eta_{CT}$ (where $\xi_{FE,CT}$ is the fraction of absorbed photon density that results in FE or CT formation and $\eta_{FE,CT}$ is the FE or CT exciton dissociation efficiency over the entire exciton lifetime). We solved numerically a system of coupled differential equations to simulate the photocurrent resulting from the drift of photogenerated charge carriers under applied electric field in the presence of electron and hole trapping, hole detrapping, and Langevin and trap-assisted recombination pathways.[10] Parameters describing charge photogeneration, transport, and trapping were varied to achieve best possible fits to the experimental data. Examples of fits are included in Figs. 2(a) and S4; contributions of SSC, FE, and CT pathways to TPCs are shown in Fig. S5; fit parameters pertinent to charge photogeneration (ξ_{SSC} and $\xi_{FE,CT}\eta_{FE,CT}$) are summarized in Figs. 2(c)–2(e); additional fit parameters can be found in Table S1.[23]

These simulations revealed that ξ_{SSC} is the main parameter responsible for the trends in I_{pk} observed in Fig. 2(b).[23] In ADT-TES-F/PCBM films, ξ_{SSC} increased from $\xi_{SSC} = 0.036$ in pristine donor films to $\xi_{SSC} = 0.195$ in ADT-TES-F/PCBM blends at 10 wt. % PCBM, followed by a decrease at higher concentrations (Fig. 2(c)). In contrast, in composites with Pn-TIPS-F8 and IF-Mes acceptors, ξ_{SSC} gradually decreased with the acceptor concentration, a trend similar to experimental observations in Fig. 2(b). The total
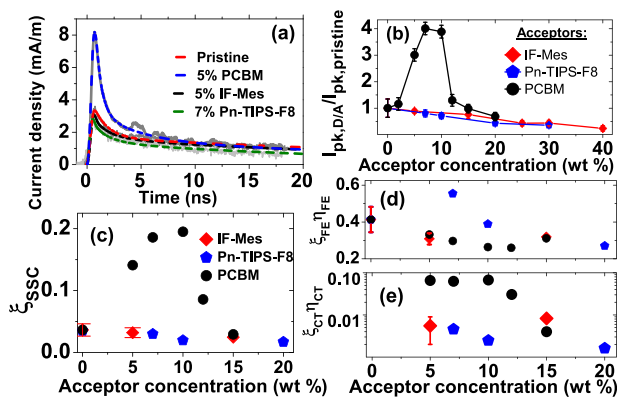

FIG. 2. (a) Transient photocurrents measured in pristine ADT-TES-F donor and various D/A films at 50 kV/cm. Dashed and dotted colored lines represent numerically simulated photocurrents. (b) Peak photocurrent at 50 kV/cm, normalized by that in pristine ADT-TES-F films, as a function of acceptor concentration for the D/A blends with three different acceptors. (c)–(e) Efficiency of (c) ultrafast charge separation ξ_{SSC} and of charge photogeneration via FE (d) and CT exciton (e) dissociation extracted from numerical modeling of the measured photocurrents in various samples. The legends for (d) and (e) are omitted for clarity, but are identical to (c). Error bars are included for several concentrations to illustrate sample-to-sample variation in the fit parameters.
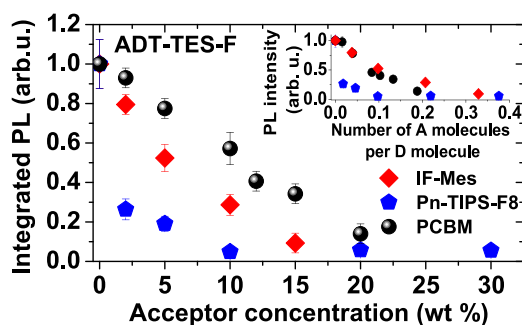
FIG. 3. Integrated PL spectra of the ADT-TES-F donor in D/A blends, normalized by that of pristine ADT-TES-F films, as a function of acceptor concentration. Inset shows the same data re-plotted as a function of the number of acceptor molecules (A) per donor (D) molecule.
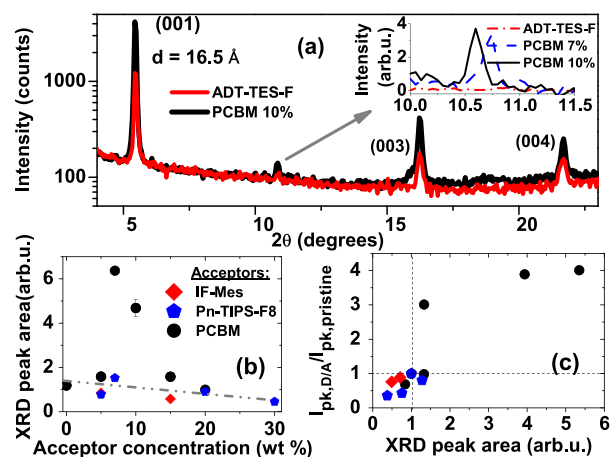

FIG. 4. (a) XRD results for out-of-plane structures in pristine ADT-TES-F and ADT-TES-F/PCBM 10 wt. % films. Inset shows a magnified view of the peak due to PCBM crystallization in D/A films with 7 wt. % and 10 wt. % of PCBM. Data from a pristine ADT-TES-F film in the same 2θ region are also included. (b) The (001) donor peak area obtained in different samples. The line provides a guide for the eye. (c) Peak photocurrent normalized by that in pristine ADT-TES-F films as a function of the (001) donor peak area normalized by that in pristine ADT-TES-F films for the D/A blends studied. The legend for (c) is identical to (b).

contribution of FE dissociation to the photocurrent ($\xi_{FE}\eta_{FE}$ in Fig. 2(d)) did not significantly depend on the acceptor, which indicates that this charge generation process occurs inside the ADT-TES-F donor domains and is only slightly affected by the presence of the D/A interfaces. In all D/A blends, the CT exciton dissociation ($\xi_{CT}\eta_{CT}$ in Fig. 2(d)) contributed a relatively small percentage of all photogenerated charge carriers (Figs. 2(d) and S5).

Next, we sought a physical explanation for the observed effects of acceptor addition on the ultrafast charge carrier separation efficiency ξ_{SSC} in Fig. 2(c). In order to account for acceptor-dependent differences in, e.g., the extent of the D/A interface, D/A packing at the D/A interface, and the density and energetics of the acceptor states,[13] we quantified donor PL quenching due to CT from the excited donor to acceptor molecules. The integrated donor PL spectra are shown as a function of acceptor wt. % concentration (Fig. 3, main) and as a function of the number of acceptor molecules per donor molecule (Fig. 3, inset). The conclusions from these plots are consistent: CT was most efficient in the case of the Pn-TIPS-F8 acceptor, the difference especially pronounced at acceptor concentrations below 10 wt. %. This indicates efficient mixing of the Pn-TIPS-F8 and ADT-TES-F molecules, facilitated by the similarity of their solid-state packing motifs. Fluorescence imaging of ADT-TES-F/Pn-TIPS-F8 films supports this observation (Figs. S3(a)–S3(b)). The donor PL quenching was considerably weaker, but followed the same trend, in D/A blends with IF-Mes and PCBM acceptors (inset of Fig. 3), suggesting segregation of D and A clusters up to at least 15 wt. % acceptor concentration (Figs. S2(c)–S2(d)). Comparison between results in Figs. 2 and 3 suggests that (i) the presence of well-mixed D/A regions, which leads to exciplex formation in ADT-TES-F/Pn-TIPS-F8 blends, does not improve the ultrafast charge carrier separation efficiency ξ_{SSC} and (ii) there is no correlation between the efficiency of CT measured via donor PL quenching (Fig. 3) and of fast charge carrier photogeneration (Fig. 2(b)).

The mechanisms of ultrafast charge carrier separation in organic semiconductors and their D/A blends have been extensively discussed in the literature.[3,26,27] Most recently, the importance of local crystallinity of donor and acceptor domains, which promote charge delocalization, has been emphasized.[2,4,28] For BHJs involving polymer donors, crystallinity of acceptor domains, which promote electron

delocalization specifically, was found to be the dominant factor. In particular, the crystallinity of fullerene acceptor regions occurring at high acceptor loading (typically above 25 wt. %) has been identified as one of the major reasons for the high performance of fullerenes as acceptors.[2] In our case, ultrafast charge separation with an efficiency ξ_{SSC} of up to 10% was observed even in pristine donor films, depending on the film preparation and experimental conditions,[10,29] and thus far only the addition of a fullerene acceptor has led to improvement in ξ_{SSC}, whereas other acceptors inhibited this channel of charge photogeneration.[6–9] Clues for the cause of this behavior are provided by the XRD data shown in Fig. 4. In all films, peaks at 5.4° (001), 16.3° (003), and 21.7° (004) were observed, confirming the crystalline nature of our films with a vertical d-spacing of 16.6 Å, characteristic of the ADT-TES-F donor (Fig. 4(a)).[15,30] Addition of Pn-TIPS-F8 and IF-Mes acceptors led to an overall reduction in the crystallinity of ADT-TES-F donor, here quantified by using the area under the (001) peak (Fig. 4(b)), and no formation of crystalline acceptor domains could be detected. Interestingly, addition of PCBM in concentrations of up to 10 wt. % led to a dramatic enhancement of the *donor* crystallinity (Fig. 4(b)),[31] correlated with the enhancement in I_{pk} (Figs. 2(b) and 4(c)). Additionally, in samples with 7 and 10 wt. % PCBM, a small peak was observed at 10.7° and 10.8°, respectively (Fig. 4(a), inset), due to crystallization of the PCBM.[4] As the PCBM concentration further increased, the ADT-TES-F donor crystallinity, as well as I_{pk} (Fig. 4(c)), decreased, and the peak due to PCBM crystallite formation could not be detected. These results may suggest that hole delocalization due to crystallinity of the ADT-TES-F donor is the dominant factor in ultrafast charge carrier separation in pristine ADT-TES-F films and ADT-TES-F-based D/A blends, and that the efficiency of this process can be further improved by electron delocalization in a crystalline acceptor.

In summary, we examined charge carrier photogeneration in small-molecule organic BHJs with a high-mobility

crystalline donor and three different acceptor molecules. Up to a factor of 4 enhancement in ultrafast charge carrier separation efficiency was observed in BHJs with PCBM added in concentrations of up to 10 wt. %. This was attributed to increased donor crystallinity, further assisted by crystallization of the PCBM acceptor, which may enhance hole and electron delocalization, respectively. In contrast, the addition of Pn-TIPS-F8 and IF-Mes led to a reduction in charge carrier photogeneration efficiencies, correlated with decreased donor crystallinity, which may reduce hole delocalization without improving electron delocalization.

[1] *Handbook of organic materials for optical and (opto)electronic devices*, 1st ed., edited by O. Ostroverkhova (Woodhead Publishing Limited, Cambridge, UK, 2013).

[2] S. D. Dimitrov and J. R. Durrant, Chem. Mater. **26**, 616 (2014).

[3] S. Gélinas, A. Rao, A. Kumar, S. L. Smith, A. W. Chin, J. Clark, T. S. van der Poll, G. C. Bazan, and R. H. Friend, Science **343**, 512 (2014).

[4] B. Bernardo, D. Cheyns, B. Verreet, R. Schaller, B. Rand, and N. Giebink, Nat. Comm. **5**, 3245 (2014).

[5] L. G. Kaake, Y. Sun, G. C. Bazan, and A. J. Heeger, Appl. Phys. Lett. **102**, 133302 (2013).

[6] M. J. Kendrick, A. Neunzert, M. M. Payne, B. Purushothaman, B. D. Rose, J. E. Anthony, M. M. Haley, and O. Ostroverkhova, J. Phys. Chem. C **116**, 18108 (2012).

[7] K. Paudel, B. Johnson, A. Neunzert, M. Thieme, B. Purushothaman, M. M. Payne, J. E. Anthony, and O. Ostroverkhova, J. Phys. Chem. C **117**, 24752 (2013).

[8] J. Day, A. D. Platt, O. Ostroverkhova, S. Subramanian, and J. E. Anthony, Appl. Phys. Lett. **94**, 013306 (2009).

[9] A. D. Platt, M. J. Kendrick, M. Loth, J. E. Anthony, and O. Ostroverkhova, Phys. Rev. B **84**, 235209 (2011).

[10] B. Johnson, M. Kendrick, and O. Ostroverkhova, J. Appl. Phys. **114**, 094508 (2013).

[11] B. Walker, C. Kim, and T.-Q. Nguyen, Chem. Mater. **23**, 470 (2011).

[12] R. J. Kline, S. D. Hudson, X. Zhang, D. J. Gundlach, A. J. Moad, O. D. Jurchescu, T. N. Jackson, S. Subramanian, J. E. Anthony, M. F. Toney, and L. J. Richter, Chem. Mater. **23**, 1194 (2011).

[13] T. Liu and A. Troisi, Adv. Mater. **25**, 1038 (2013).

[14] M. Schubert, B. A. Collins, H. Mangold, I. A. Howard, W. Schindler, K. Vandewal, S. Roland, J. Behrends, F. Kraffert, R. Steyrleuthner, Z. Chen, K. Fostiropoulos, R. Bittl, A. Salleo, A. Facchetti, F. Laquai, H. W. Ade, and D. Neher, Adv. Funct. Mater. **24**, 4068 (2014).

[15] S. K. Park, D. A. Mourey, S. Subramanian, J. E. Anthony, and T. N. Jackson, Appl. Phys. Lett. **93**, 043301 (2008).

[16] D. J. Gundlach, J. E. Royer, S. K. Park, S. Subramanian, O. D. Jurchescu, B. H. Hamadani, A. J. Moad, R. J. Kline, L. C. Teague, O. Kirillov, C. A. Richter, J. G. Kushmerick, L. J. Richter, S. R. Parkin, T. N. Jackson, and J. E. Anthony, Nat. Mater. **7**, 216 (2008).

[17] A. D. Platt, J. Day, S. Subramanian, J. E. Anthony, and O. Ostroverkhova, J. Phys. Chem. C **113**, 14006 (2009).

[18] A. G. Fix, P. E. Deal, C. L. Vonnegut, B. D. Rose, L. N. Zakharov, and M. M. Haley, Org. Lett. **15**, 1362 (2013).

[19] T. M. Clarke and J. R. Durrant, Chem. Rev. **110**, 6736 (2010).

[20] J. D. Servaites, M. A. Ratner, and T. J. Marks, Eng. Env. Sci. **4**, 4410 (2011).

[21] X.-Y. Zhu, J. Phys. Chem. Lett. **5**, 2283 (2014).

[22] S. Subramanian, S. K. Park, S. R. Parkin, V. Podzorov, T. N. Jackson, and J. E. Anthony, J. Am. Chem. Soc. **130**, 2706 (2008).

[23] See supplementary material at http://dx.doi.org/10.1063/1.4891758 for optical absorption, PL spectra, and PL images as well as details and results of numerical simulations of transient photocurrents.

[24] M. Wójcik and M. Tachiya, J. Chem. Phys. **130**, 104107 (2009).

[25] C. L. Braun, J. Chem. Phys. **80**, 4157 (1984).

[26] L. G. Kaake, J. J. Jasieniak, R. C. Bakus, G. C. Welch, D. Moses, G. C. Bazan, and A. J. Heeger, J. Am. Chem. Soc. **134**, 19828 (2012).

[27] K. Vandewal, S. Albrecht, E. T. Hoke, K. R. Graham, J. Widmer, J. D. Douglas, M. Schubert, W. R. Mateker, J. T. Bloking, G. F. Burkhard, A. Sellinger, J. M. J. Frechet, A. Amassian, M. K. Riede, M. D. McGehee, D. Neher, and A. Salleo, Nat. Mater. **13**, 63 (2014).

[28] A. E. Jailaubekov, A. P. Willard, J. R. Tritsch, W.-L. Chan, N. Sai, R. Gearba, L. G. Kaake, K. J. Williams, K. Leung, P. J. Rossky, and X.-Y. Zhu, Nat. Mater. **12**, 66 (2012).

[29] B. Johnson, K. Paudel, M. J. Kendrick, and O. Ostroverkhova, Proc. SPIE **8830**, 88301S (2013).

[30] Y. S. Chung, N. Shin, J. Kang, Y. Jo, V. M. Prabhu, S. K. Satija, R. J. Kline, D. M. DeLongchamp, M. F. Toney, M. A. Loth, B. Purushothaman, J. E. Anthony, and D. Y. Yoon, J. Am. Chem. Soc. **133**, 412 (2011).

[31] A. Sharenko, M. Kuik, M. F. Toney, and T.-Q. Nguyen, Adv. Funct. Mater. **24**, 3543 (2014).